Crystal growth and Judd-Ofelt analysis of novel Tm^{3+}-doped BaCaBO$_3$F crystal

WANG ZHAO[a,*], WEIWEI ZHOU[b], MINGJUN SONG[c], GUOFU WANG[d], JIANMING DU[a], HAIJUN YU[a], JINGXIA CHEN[a]

[a]*Department of Physics, Huainan Normal University, Huainan, Anhui 232001, P. R. China*
[b]*Department of Chemistry & Chemical Engineering, Huainan Normal University, Huainan, Anhui 232001, P. R. China*
[c]*College of Chemical Engineering, Weifang University, Weifang, Shandong 261061, P. R. China*
[d]*Key Laboratory of Optoelectronic Materials Chemistry and Physics, Fujian Institute of Research on the Structure of Matter, Chinese Academy of Sciences, Fuzhou, Fujian 350002, P. R. China*

Tm^{3+}-doped BaCaBO$_3$F crystals have been grown by the Czochralski method. The grown crystals have been inclined to crack along the (001) plane due to the layered structure. Polarization absorption spectra have been recorded at room temperature. The peak absorption cross-sections around 800 nm are 0.84×10^{-20} cm^2 with full width at half maximum (FWHM) of 17.4 nm for π-polarization and 1.18×10^{-20} cm^2 with FWHM of 16.5 nm for σ-polarization, respectively. The Judd-Ofelt theory, extended to anisotropic system, has been applied to evaluate the spectroscopic parameters relevant for laser applications, such as phenomenological intensity parameters, spontaneous transition probabilities, branching ratios and radiative lifetimes.

1. Introduction
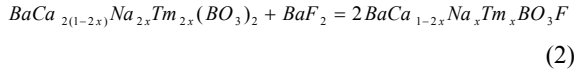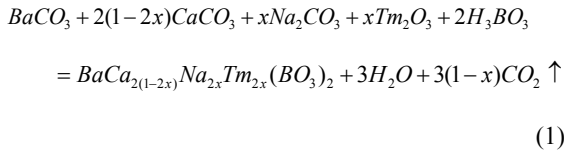
Laser radiation around 2.0 μm has important applications, such as for coherent laser radar, remote sensing and medical equipment [1-3]. Tm^{3+}-doped crystals are primarily employed as laser sources in this spectral region. Major advantages with Tm^{3+}-doped active matrices include the availability of AlGaAs laser diode pumping via the ^{3}H$_6$ → ^{3}H$_4$ transition at ~800 nm, the efficient near infrared laser operation associated with a favorable cross-relaxation process (^{3}H$_4$ + ^{3}H$_6$ → ^{3}F$_4$ + ^{3}F$_4$), and a tunability near 2.0 μm. Therefore, Tm^{3+}-doped crystalline materials have been investigated extensively and deeply [4-11].

BaCaBO$_3$F crystallizes in the hexagonal system with space group $P\bar{6}2m$ and unit cell parameters: a = 9.049 Å and c = 4.326 Å [12]. Its basic structural units are the triangular (BO$_3$)$^{3-}$ groups responsible for the nonlinear optical effect. In 1996, Yb^{3+}:BaCaBO$_3$F were assessed as a new laser crystal with potential for self-frequency doubling [13]. The Yb^{3+}:BaCaBO$_3$F crystal was characterized by long energy storage time of Yb^{3+}, large crystal field splittings for Yb^{3+}, and the combined second-harmonic generation and laser features available from the crystal. With a Ti:sapphire pumping source, slope efficiency up to 38% was obtained for the fundamental laser output (1034 nm). Recently, BaCaBO$_3$F crystals with large size were grown by the Kyropoulos and Czochralski methods, and the detailed linear and nonlinear optical properties of this material were presented [14-16]. In this work, the growth and polarized absorption spectra of the Tm^{3+}:BaCaBO$_3$F crystal are reported. The Judd–Ofelt analysis, which is crucial to understand the relationships between host and Tm^{3+} emission properties, has been applied to predict the spectroscopic parameters relevant for laser applications.

2. Experimental

BaCaBO$_3$F melts congruently [14, 16]. According, the Tm^{3+}:BaCaBO$_3$F crystal was grown by the Czochralski method. The chemicals used were Tm$_2$O$_3$ with purity of 99.99%, and BaCO$_3$, CaCO$_3$, Na$_2$CO$_3$, H$_3$BO$_3$, BaF$_2$ with AR grade. Since Tm^{3+} replaced the divalent cation Ca^{2+}, Na$^+$ was codoped as a charge compensator element so as to ensure the lattice electric neutrality and to increase the efficiency of dopant incorporation. In order to avoid the formation of Ba and/or Ca peroxide which attacked the crucible, a two-step process was adopted for preparing a melt from which a crystal could be grown [12], as described by the following reaction:

$$BaCO_3 + 2(1-2x)CaCO_3 + xNa_2CO_3 + xTm_2O_3 + 2H_3BO_3$$

$$= BaCa_{2(1-2x)}Na_{2x}Tm_{2x}(BO_3)_2 + 3H_2O + 3(1-x)CO_2 \uparrow$$

(1)

$$BaCa_{2(1-2x)}Na_{2x}Tm_{2x}(BO_3)_2 + BaF_2 = 2BaCa_{1-2x}Na_xTm_xBO_3F$$

(2)

where $x = 0.02$. Crystal pulling was performed in N_2 atmosphere using a platinum crucible. The detailed crystal growth procedure was described elsewhere [13, 16]. Similar to the Yb^{3+}:$BaCaBO_3F$ crystal [13], the Tm^{3+}:$BaCaBO_3F$ crystal cracks easily, which can be related to layered structure. In the structure of $BaCaBO_3F$, (BO_3) groups and Ca atoms link each other to form layers along (001) plane, and the bond between the layers consists of Ba and F atoms [16], as shown in Fig. 1. Owing to the large distance between layers (4.3257 Å), the contact between adjacent layers is weak, so the crystal is apt to fracture along (001) plane.
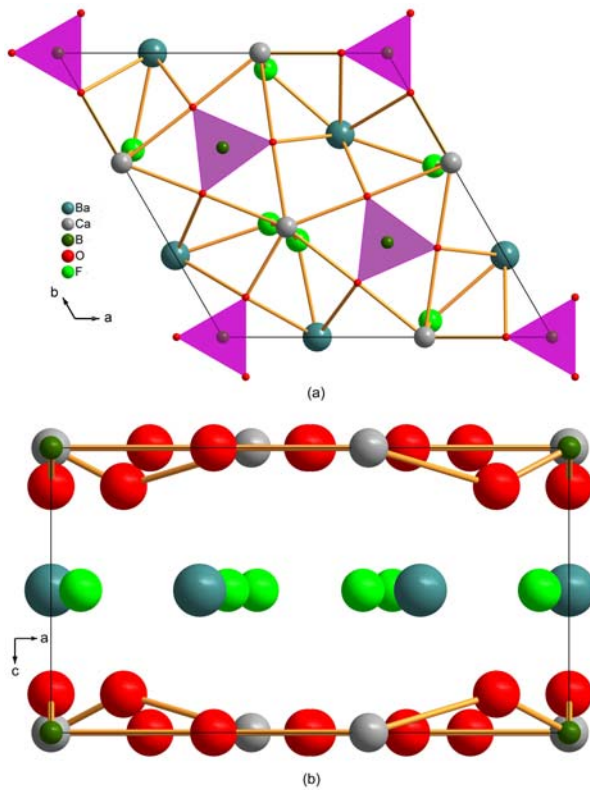

Fig. 1. Crystal structure of $BaCaBO_3F$.

The concentration of Tm^{3+} in the $BaCaBO_3F$ crystal was measured by inductively coupled plasma and atomic emission spectrometry (Ultima2, Jobin–Yvon). A 1.98 mm thick plate sample cut from the as-grown crystal with the c-axis contained in its main faces was applied to the σ ($E \perp c$, $k \perp c$) and π ($E // c$, $k \perp c$) polarized spectral measurements, where E, k, and c are the electric field,

wave vector, and optical axis of the uniaxial crystal, respectively. The polarized absorption spectra were recorded by a UV/VIS/NIR Spectrometer (Lambda900, Perkin–Elmer).

3. Results and discussions

3.1 Efficient segregation coefficient

The Tm^{3+} concentration in the Tm^{3+}:$BaCaBO_3F$ crystal have been determined to be 3.48 wt.% (5.14×10^{20} cm^{-3}). The segregation coefficient K of Tm^{3+} in the crystal can be expressed as:

$$K = C_{sol} / C_{liq}$$

(3)

where C_{sol} and C_{liq} are the concentrations of Tm^{3+} in the solid and liquid phases, respectively. Thus, the segregation coefficient K of Tm^{3+} in $BaCaBO_3F$ crystal are 2.63.

3.2 Absorption spectra

Fig. 2 illustrates the polarized absorption spectra of the Tm^{3+}:$BaCaBO_3F$ crystal at room temperature. The baselines in the spectra, which are caused by the Fresnel reflection of the crystal surface and the defects in the crystal, have been corrected. All the absorption bands are attributed to the transitions of Tm^{3+} ions from the ground state $^3H_6$ to the excited state J' manifolds, which are also marked in Fig. 2. As can be seen, the absorption spectra show pronounced polarization dependence due to the anisotropy of the crystal, with σ-polarization giving stronger line. The most interesting feature in the absorption spectra is the strong absorption band around 800 nm corresponding to the $^3H_6 \rightarrow {}^3H_4$ transition, which coincides with wavelength of radiation from GaAlAs diode laser. For the σ-polarized spectrum, the peak absorption is situated at 793 nm with an absorption cross-section of 1.18×10^{-20} cm^2 and full width at half the maximum (FWHM) of 16.5 nm, while for the π-polarized spectrum, the most intense absorption is located at 796 nm with an absorption cross-section of 0.84×10^{-20} cm^2 and FWHM of 17.4 nm. The maximum value of absorption cross-sections approaches those of Tm^{3+}:YAG (0.75×10^{-20} cm^2) [17], Tm^{3+}:YVO_4 (2.50×10^{-20} cm^2 for π-polarization) [18] and Tm^{3+}:$GdAl(BO_3)_4$ (1.75×10^{-20} cm^2 for π-polarization) [11]. The FWHM is much larger than those of Tm^{3+}:YVO_4 (5.0 nm) [18] and Tm^{3+}:$KYb(WO_4)_2$ (3.5 nm) [19] and comparable to those of Tm^{3+}:$GdAl(BO_3)_4$ (13.0 nm) [11], and Tm^{3+}:$LiLuF_4$ (20.0 nm) [7]. Considering that the wavelength temperature coefficient is about 0.3 nm/°C and the spectral width is about 2.0 nm for commonly commercial diode lasers, such bandwidth is suitable for diode pumping, since it is not crucial to temperature stability of the output wavelengths of diode laser.
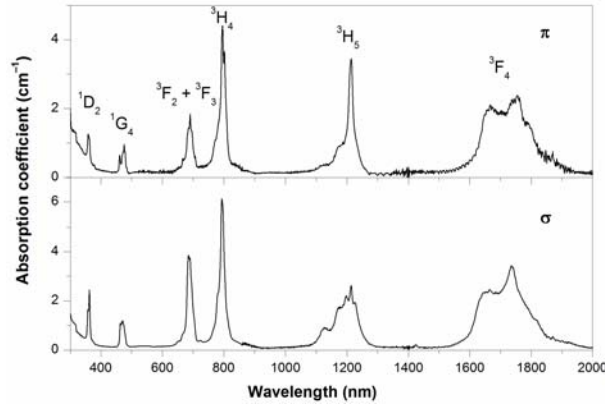
Fig. 2. Polarized absorption spectra of the Tm³⁺:BaCaBO₃F crystal at room temperature.

3.3 Judd–Ofelt anylysis

The Judd–Ofelt theory has become standard tool for evaluating the spectroscopic parameters of rare-earth ions in crystals and glasses [20, 21]. The calculation procedure is similar to those of Refs. [22-24], and we will make a brief description giving the equations used in our analysis.

In the framework of the Judd–Ofelt theory, the line strength of the electric-dipole transition between an initial state J and a final state J' can be expressed as:

$$S_q^{ed}(J \to J') = \sum_{t=2,4,6} \Omega_t \left| \left\langle [L,S]J \left\| U^{(t)} \right\| [L',S']J' \right\rangle \right|^2 \quad (4)$$

where the subscript q indicates the polarization of the absorption spectra, and the three phenomenological intensity parameters Ω_2, Ω_4, Ω_6 convey the influence of the host on the transition probabilities, since they incorporate the crystal-field parameters, interconfigurational radial integrals, the interaction between the central ion and the immediate environment [8]. $\left\langle [L,S]J \left\| U^{(t)} \right\| [L',S']J' \right\rangle$ are the doubly reduced matrix elements of unitary tensor operators, which are almost independent of the ion environment. These matrix elements, calculated in the intermediate coupling scheme, have been tabulated in Refs. [8, 25].

On the other hand, the line strength for the magnetic dipole transition between an initial state J and a final state J' is given by:

$$S_q^{md}(J \to J') = \left(\frac{h}{4\pi mc}\right)^2 \left| \left\langle [L,S]J \left\| L+2S \right\| [L',S']J' \right\rangle \right|^2 \quad (5)$$

where $L+2S$ is the magnetic dipole operator. In view of the selection rules: $\Delta S = \Delta L = 0$, $\Delta J = 0, \pm1$ ($0 \leftrightarrow 0$ forbidden) in the Russel–Saunder limit, the magnetic dipole transitions only contribute to the $^3H_6 \to {}^3H_5$ absorption band of Tm³⁺ here. The values of S_{md} are usually small and are insensitive to the host, so we have employed the values supplied in Ref. [26].

According to the Judd–Ofelt theory, the line strength of the electric-dipole transition of the $J \to J'$ transition (J represents the ground state $^3H_6$ here) can also be extracted

experimentally from the corresponding room-temperature absorption spectra by the following formula:

$$S_q^{exp}(J \to J') = \frac{9n}{(n^2+2)^2}\left[\frac{3hc(2J+1)}{8\pi^3 e^2 \bar{\lambda} N_0} \int \alpha_q(\lambda)d\lambda - nS_q^{md}(J \to J') \right] \quad (6)$$

where h is the Planck constant, m and e are the electron mass and charge, c is the velocity of light, N_0 is the concentration of Tm³⁺ in the crystal, $\alpha_q(\lambda)$ is the absorption coefficient and $\int \alpha_q(\lambda)d\lambda$ is the integrated absorption coefficient for each absorption band. The refractive indexes n are obtained from the Sellmeier equations established for BaCaBO₃F crystal reported in Ref. [16]:

$$n_o^2 = 2.71455 + \frac{0.01871\lambda^2}{\lambda^2 - 0.01730} - 0.00906\lambda^2 \quad (7)$$

$$n_e^2 = 2.55994 + \frac{0.01599\lambda^2}{\lambda^2 - 0.01752} - 0.00528\lambda^2 \quad (8)$$

where λ stands for the wavelength (unit: μm). In the subsequent calculation, the values of n_o and n_e are used for the σ- and π-polarized spectra, respectively.

Thus, the intensity parameters Ω_t (t = 2, 4, 6) are estimated by a least-square fitting between equations (4) and (6). Making use of equation (4) and the obtained Ω_t value, the calculated line strengths S_{cal} can be determined. Then, the values of experimental and calculated line strengths are listed in Table 1. To justify the results obtained, the root-mean-square deviation of the experimental and calculation line strengths is introduced, which is defined by:

$$rms\,\Delta S_q = \sqrt{\frac{\sum_{i=1}^{N}(S_q^{exp} - S_q^{cal})^2}{N_{tr} - N_{par}}} \quad (9)$$

where N_{tr} is the number of transitions and N_{par} is the number of parameters. A measurement of the relative error defined as $rms\ error = rms\ \Delta S / rms\ S$ is also carried out. The values of the $rms\ error$ are 4.4 % and 5.7 % for π- and σ-polarizations, respectively, which are in the typical error range of Judd–Ofelt fitting and indicate good agreement between the calculated and experimental results.

Table 1. Experimental and calculated line strengths of Tm³⁺ in the BaCaBO₃F crystal (in units of 10⁻²⁰ cm²).

Transitions	π-polarization		σ-polarization	
$^3H_6 \to$	S_{exp}	S_{cal}	S_{exp}	S_{cal}
$^3F_4$	4.05	4.05	5.34	5.41
$^3H_5$	1.35	1.24	2.27	2.13
$^3H_4$	1.81	1.85	2.95	2.89
$^3F_2 + {}^3F_3$	0.92	0.95	2.05	2.16
$^1G_4$	0.41	0.37	0.63	0.49
$^1D_2$	0.33	0.37	0.67	0.56
$rms\,\Delta S$	0.09		0.16	

Wang Zhao, Weiwei Zhou, Mingjun Song, Guofu Wang, Jianming Du, Haijun Yu, Jingxia Chen

Table 2. The intensity parameters of Tm^{3+}-doped crystals (in units of 10^{-20} cm^2).

Crystals	Ω_2	Ω_4	Ω_6	Ω_4/Ω_6	Refs.
Tm^{3+}:YAG	0.70	1.20	0.50	2.40	[27]
Tm^{3+}:YVO$_4$	7.81	1.03	1.14	0.90	[6]
Tm^{3+}:GdAl$_3$(BO$_3$)$_4$	4.54	2.55	3.39	0.75	[11]
Tm^{3+}:Ca$_4$GdO(BO$_3$)$_4$	1.92	0.15	0.63	0.24	[10]
Tm^{3+}:Sr$_3$Y(BO$_3$)$_3$	2.16	0.66	2.07	0.32	[28]
Tm^{3+}:BaCaBO$_3$F	7.59^σ	1.31^σ	1.59^σ	0.83^σ	This
	5.93^π	1.00^π	0.58^π	1.74^π	work
	7.04^{eff}	1.21^{eff}	1.25^{eff}	0.97^{eff}	

The effective intensity parameters, which are defined as $\Omega_{eff} = (\Omega_\pi + 2\Omega_\sigma)/3$, are also obtained. In Table 2, the Judd–Ofelt parameters that result from the above mentioned analysis are compared with the values obtained for several laser crystals containing Tm^{3+}. It is observed that the effective intensity parameters for the Tm^{3+}:BaCaBO$_3$F crystal is similar to that for the Tm^{3+}:YVO$_4$ crystal in which an efficient laser output around 2.0 μm has been demonstrated [29]. The spectroscopic quality factor, $X = \Omega_4/\Omega_6$, first introduced by Kaminiskii and co-workers [30], is also an important laser characteristic in predicting the stimulated emission in laser active medium. The spectroscopic quality factor for Tm^{3+} in the BaCaBO$_3$F is determined to be 0.97, which fall within the range of 0.24–2.40 for Tm^{3+}-doped different hosts listed in Table 2.

Once the intensity parameters have been obtained, the spontaneous emission probabilities $A(J \to J')$ between the excited state J and terminating state J' can be calculated by the following expressions in terms of the S_{ed} and S_{md} strengths:

$$A_q(J \to J') = A_q^{ed}(J \to J') + A_q^{md}(J \to J') \quad (10)$$

$$A_q^{ed}(J \to J') = \frac{64\pi^4 e^2}{3h\overline{\lambda}_{em}^3(2J+1)} \frac{n_q(n_q^2+2)^2}{9} S_q^{ed}(J \to J') \quad (11)$$

$$A_q^{md}(J \to J') = \frac{64\pi^4 e^2 n_q^3}{3h\overline{\lambda}_{em}^3(2J+1)} S_q^{md}(J \to J') \quad (12)$$

where $\overline{\lambda}_{em}$ is the mean wavelength of emission bands, A_{ed} and A_{md} are the spontaneous emission probabilities of the electric dipole (*ed*) and magnetic dipole (*md*) transitions, respectively.

The fluorescence branching ratio from the same excited state J can be determined from the spontaneous emission probability according to the relations:

$$\beta_q(J \to J') = \frac{A_q(J \to J')}{\sum_{J'} A_q(J \to J')} \quad (13)$$

The radiative lifetime for any specific excited state J is the reciprocal of the total spontaneous emission probability. For a uniaxial crystal, the total spontaneous emission probability is expressed as:

$$A_{total} = \frac{\sum_{J'} A_\pi(J \to J') + 2\sum_{J'} A_\sigma(J \to J')}{3} \quad (14)$$

$$\tau_r = \frac{1}{A_{total}} \quad (15)$$

The calculated electric and magnetic dipole spontaneous emission probabilities, radiative lifetimes, and branching ratios for the main emission transitions of Tm^{3+} in the BaCaBO$_3$F crystal, are summarized in Table 3.

Table 3. Calculated spontaneous emission probabilities, branching ratios, and radiative lifetimes of Tm^{3+} in the BaCaBO$_3$F crystal.

Transitions		λ_{em} (nm)	π-polarization			σ-polarization			τ_{rad} (μs)
			A_{ed} (s^{-1})	A_{md} (s^{-1})	β	A_{ed} (s^{-1})	A_{md} (s^{-1})	β	
$^1G_4 \to$	$^3H_6$	470	1107.1	0	0.533	1612.0	0	0.467	334.2
	$^3F_4$	646	92.4	8.5	0.049	207.8	9.3	0.063	
	3H$_5$	763	506.2	95.4	0.289	1055.0	104.2	0.336	
	$^3H_4$	1177	209.0	21.7	0.111	356.9	23.6	0.110	
	$^3F_3$	1494	27.0	2.4	0.014	62.9	2.6	0.019	
	$^3F_2$	1634	9.0	0	0.004	15.4	0	0.004	
$^3H_4 \to$	$^3H_6$	784	1163.0	0	0.891	1990.6	0	0.904	525.3
	$^3F_4$	1432	102.5	15.6	0.090	163.7	16.9	0.082	
	$^3H_5$	2166	16.2	7.9	0.019	23.4	8.5	0.014	
$^3H_5 \to$	$^3H_6$	1225	163.7	58.7	0.983	310.2	64.0	0.980	3031.1
	$^3F_4$	4226	3.6	0.1	0.017	7.5	0.1	0.020	
$^3F_4 \to$	$^3H_6$	1725	233.0	0	1.000	340.5	0	1.000	3282.4

4. Conclusions

Tm^{3+}-doped $BaCaBO_3F$ crystals have been grown by the Czochralski method. The grown crystals have a tendency to crack along the (001) plane because of the layered structure. The crystal is characterized by a wide absorption bandwidth (~17 nm) at the pumping laser wavelength such that wavelength requirements imposed on laser diodes are relaxed to a great extent. The maximum absorption cross-sections around 800 nm are 0.84×10^{-20} cm^2 for π-polarization and 1.18×10^{-20} cm^2 for σ-polarization, respectively. Based on the analysis of the polarized absorption spectra in the framework of the Judd–Ofelt theory, the main spectroscopic characteristics, such as phenomenological intensity parameters, spontaneous transition probabilities, branching ratios and radiative lifetimes, have been determined.

References

[1] F. Cornacchia, A. Toncelli, M. Tonelli, Prog. Quant. Electron. **33**, 61 (2009).
[2] A. Godard, C. R. Physique **8**, 1100 (2007).
[3] B. M. Walsh, Laser Phys. **19**, 855 (2009).
[4] L. H. Zeng, J. Xu, L. B. Su, H. J. Li, W. Ryba-Ramanowski, R. Lisiecki, P. Solarz, Appl. Phys. Lett. **96**, 121908 (2010).
[5] J. F. Tang, Y. J. Chen, Y. F. Lin, X. H. Gong, J. H. Huang, Z. D. Luo, Y. D. Huang, J. Opt. Soc. Am. B **27**, 1769 (2010).
[6] R. Lisiecki, P. Solarz, G. Dominiak-Dzik, W. Ryba-Romanowski, M. Sobczyk, P. Černý, J. Šulc, H. Jelínková, Y. Urata, Phys. Rev. B **74**, 035103 (2006).
[7] J. Xiong, H. Y. Peng, C. C. Zhao, Y. Hang, L. H. Zhang, M. Z. He, X. M. He, G. Z. Chen, Laser Phys. Lett. **6**, 868 (2009).
[8] B. M. Walsh, N. P. Barnes, B. D. Bartolo, J. Appl. Phys. **83**, 2772 (1998).
[9] J. M. Cano-Terres, M. D. Serrano, C. Zaldo, M. Rico, X. Mateos, J. H. Liu, U. Griebner, V. Petrov, F. J. Valle, M. Galán, G. Viera, J. Opt. Soc. Am. B **23**, 2494 (2006).
[10] G. Dominiak-Dzik, W. Ryba-Romanowski, S. Golab, A. Pajaczkowska, J. Phys.: Condens. Matter **12**, 5495 (2000).
[11] G. H. Jia, C. Y. Tu, J. F. Li, X. A. Lu, Z. J. Zhu, Z. Y. You, Y. Wang, B. C. Wu, J. Appl. Phys. **99**, 083502 (2006).
[12] D. A. Keszler, A. Akella, K. I. Schaffers, T. Alekel III, Mater. Res. Soc. Symp. Proc. **329**, 15 (1994).
[13] K. I. Schaffers, L. D. Deloach, S. A. Payne, IEEE J. Quantum Electron. **32**, 741 (1996).
[14] G. C. Zhang, H. J. Liu, X. A. Wang, F. D. Fan, P. Z. Fu, J. Cryst. Growth **289**,188 (2006).
[15] X. Wang, G. C. Zhang, Y. Zhao, F. D. Fan, H. J. Liu, P. Z. Fu, Opt. Mater. **29**, 1658 (2007).
[16] K. Xu, P. Loiseau, G. Aka, J. Cryst. Growth **311**, 2508 (2009).
[17] T. Y. Fan, G. Huber, R. L. Byer, P. Mitzscherlich, IEEE J. Quantum Electron. **24**, 924 (1988).
[18] K. Ohta, H. Saito, M. Obara, J. Appl. Phys. **73**, 3149 (1993).
[19] M. C. Pujol, F. Güell, X. Mateos, J. Gavaldà, R. Solé, J. Massons, M. Aguiló, F. Díaz, G. Boulon, A. Brenier, Phys. Rev. B **66**, 144304 (2002).
[20] B. R. Judd, Phys. Rev. **127**, 750 (1962).
[21] G. S. Ofelt, J. Chem. Phys. **37**, 511 (1962).
[22] C. Gheorghe, A. Lupei, V. Lupei, L. Gheorghe, S. Hau, J. Optoelectron. Adv. Mater. **12**, 818 (2010).
[23] A. Nistreanu, N. Enachi, M. Iovu, V. Koroli, D. Furniss, A. Seddon, J. Optoelectron. Adv. Mater. **12**, 800 (2010).
[24] P. R. Rejikumar, P. Vasudevan, S. Karthika, J. George. N. V. Unnikrishhan, J. Optoelectron. Adv. M. **12**, 1065 (2010).
[25] W. T. Carnall, P. R. Fields, K. Rajnak, J. Chem. Phys. **49**, 4424 (1968).
[26] N. Spector, R. Reisfeld, L. Boehm., Chem. Phys. Lett. **49**, 49 (1977).
[27] M. J. Weber, T. E. Varitimos, B. H. Matsinger, Phys. Rev. B **8**, 47 (1973)
[28] X. M. Meng, L. Z. Zhang, G. F. Wang, J. Alloys Compd. **481**, 354 (2009).
[29] J. J. Zayhowski, J. Harrison, C. Dill III, J. Ochoa, Appl. Opt. **34**, 435 (1995).
[30] A. A. Kaminskii, G. Boulon, M. Buoncristiani, B. Di Bartolo, A. Kornienko, V. Mironov, Phys. Status. Solidi. A **141**, 471 (1994).

_____
[*]Corresponding author: zwwwz@live.com